Regulation of human T-cell leukemia virus type 1 antisense promoter by myocyte enhancer factor-2C in the context of adult T-cell leukemia and lymphoma

Kiran K. Madugula,[1] Julie Joseph,[1] Catherine DeMarino,[2] Rashida Ginwala,[3] Vanessa Teixeira,[1,4] Zafar K. Khan,[1] Dominic Sales,[1] Sydney Wilson,[1] Fatah Kashanchi,[2] Amanda W. Rushing,[5] Isabelle Lemasson,[5] Edward W. Harhaj,[6] Murali Janakiram,[7] B. Hilda Ye[8] and Pooja Jain[1]

[1]Department of Microbiology and Immunology, Drexel University College of Medicine, Philadelphia, PA, USA; [2]Laboratory of Molecular Virology, George Mason University, Manassas, VA, USA; [3]Fox Chase Cancer Center, Thomas Jefferson University, Philadelphia, PA, USA; [4]Instituto de Ciencias Biológicas, Universidad de Pernambuco, Recife, PE, Brazil; [5]Department of Microbiology and Immunology, Brody School of Medicine, East Carolina University, Greenville, NC, USA; [6]Department of Microbiology and Immunology, Penn State College of Medicine, Hershey, PA, USA; [7]Department of Oncology, Montefiore Medical Center and [8]Department of Cell Biology, Albert Einstein College of Medicine, Bronx, NY, USA

Correspondence: P. Jain
pj27@drexel.edu

Received: June 28, 2021.
Accepted: May 18, 2022.
Prepublished: May 26, 2022.

https://doi.org/10.3324/haematol.2021.279542

Supplementary data.

Supplementary methods:

Cell lines. HTLV-1-transformed cell lines MT-2, MT-4 (1, 2), M8166 (3) and SP (HTLV-1-infected clone from PBMCs of an ATLL patient) (4) were obtained through the NIH AIDS Reagent Program (Catalog No. 237, 120, 11395 and 3059, respectively). HTLV-1-negative Jurkat cell line (E6-1, Cat No. 177) was also obtained from NIH while SLB-1 (5-8) and ATLL-derived cell lines, ATL-2S (9-11), ED-40515(-) (referred here as ATL-ED) (9, 11, 12), and ATL-55T were described previously (12, 13). Cultures were maintained in RPMI 1640 medium supplemented with L-glutamine (Atlanta Biologicals, Flowery Branch, GA), 10% fetal bovine serum (FBS, Atlanta Biologicals) and 1x Penicillin/Streptomycin (Gibco, Gaithersburg, MD) in a humidified incubator with 10% CO_2 at 37°C. SP culture was supplemented with 100 U/mL of human IL-2 (Peprotech Inc., Rocky Hill, NJ).

In addition, three NA-ATLL patient-derived $CD4^+$ T-cell lines (ATL13, ATL18, ATL21) were obtained from the Albert Einstein College of Medicine (NY, USA) and maintained in IMDM with 100 units/mL IL-2 and 20% human serum. Two additional HTLV-1-negative human T-cell lines HUT78 and OCI-Ly13.2 were cultured in RPMI with 10% FBS while the third HH line was maintained in IMDM plus 20% FBS. All cell lines were routinely tested for mycobacterium contaminants via PCR (Applied Biological Materials).

MTT cell viability/cytotoxicity assay. Prior to experiments, viability of all cell lines was assessed, and exponential phase cultures were utilized. Cells were seeded into 96-well plates at a density of 100,000 cells per well in Gibco's phenol red-free RPMI medium for 48 hours at 37°C in a humidified chamber. Cell viability was assessed using Vybrant® MTT Cell Proliferation Assay

according to the manufacturer's protocol (ThermoFisher, Waltham, MA). Following the initial 48 hr incubation, 10 μL of 12 mM MTT was added to each well, then incubated for 4 hrs at 37°C before cells were lysed in 100μL of SDS-HCl solution. Cells were incubated for another 4 hrs at 37°C before final absorbance was measured at 570 nm (Sunrise™, Tecan, NC) as a direct assessment of viable cells in each culture. Similar MTT assays were utilized to test cytotoxic effects of MC1568 in a standard 2-fold dilution method with IC_{50} calculation by Prism8 software (GraphPad).

qPCR assay for determining integrated HTLV-1 copy number. Genomic DNA (gDNA) for each cell line was obtained using DNeasy Kit (Qiagen). Integrated HTLV-1 copy number was determined by performing quantitative polymerase chain reaction (qPCR) using the SYBR green assay (Quant Studio 6 Flex, Applied Biosystems) with GAPDH as an internal control and gDNA from the HTLV-1-infected rat cell line (TARL-2) as a reference since it carries one copy of provirus per cell (14). The following primer set was used to amplify the HTLV-1 regulatory Px region: 5'-CAAAGTTAACC ATGCTTATTATCAGC-3' (forward) and 5'-ACACGTAGACTGGGTATCCGAA-3' (reverse). A standard curve for the Px region, representing integrated HTLV-1, was generated from assay results using two-fold serial dilutions of TARL-2 gDNA. The HTLV-1 copy number for each cell line was calculated from the standard curve, using the respective CT values, and divided by the estimated number of cells (1ng DNA = 151.51 diploid cells) as described in (15)

Western blotting for viral protein expression. Protein lysates were extracted from transfected cultures using Pierce RIPA Buffer supplemented with protease inhibitor cocktail

(Thermofisher Scientific) and phosphatase inhibitor Cocktail 3 (Sigma-Aldrich). Total protein concentration was measured using a BCA protein assay (Pierce, ThermoFisher) and 25-30 μg of proteins were loaded per lane in 4-15% gradient SDS-PAGE gels (Bio-Rad). Proteins were transferred onto methanol activated PVDF membranes at 4°C for 16-18 hours at 30V. Membranes were then blocked for 1 hour in 5% fat-free milk in 1xTBS plus Tween 20, washed with TBS-t Tween, and probed for target antibody. Images were read using the Gel Doc XR+ Gel Documentation System (Bio-Rad) and processed on Image Lab software. Primary antibodies used were anti-HBZ (dilution 1:1000; provided by Dr. Amanda Panfil, Ohio State University), anti-Tax LT-4 (1:2000), provided by Dr. Yuetsu Tanaka (Japan).

Measurement of HTLV-1 infectivity (p19) via ELISA. Supernatants from each cell line were collected at 48 hrs in order to quantify extracellular levels of p19 protein released by each cell line. Enzyme-linked immunosorbent assay (ELISA) was performed in duplicate for each cell line using the HTLV p19 Antigen ELISA kit (Zeptometrix), according to manufacturer's instructions. The final absorbance was measured at 450 nm (Sunrise™) and data was analyzed using the standard curve method, which was generated from serial dilutions of the standards.

Phenotyping of cell lines by FACS. Jurkat cells and three virus-producing cell lines, MT-2, MT-4 and SP, were counted and 1 x 10^6 cells were surface stained for CD3 and CD4 using fluorochrome-conjugated antibodies, AF700 and FITC, respectively. Samples were incubated for 30 mins at 4°C in the dark. For intracellular staining of Tax, cells were fixed and permeabilized with 200 μL of permeabilization buffer followed by staining using 20 μL of PE-conjugated Tax (conjugated in-house using Abcam PE conjugation kit cat: ab102918) antibody for 30 mins at 4°C

in the dark. After incubation, cells were washed twice with 1x permeabilization buffer and resuspended with staining buffer for analysis by flow cytometry using BD FACS Calibur (BD Biosciences, San Jose, CA).

Analysis of MEF-2 isoform mRNA levels by PrimeFlow™ and RT-qPCR. The PrimeFlow™ RNA assay (Affymetrix, Santa Clara, CA) is an *in-situ* hybridization assay that can detect target RNA transcripts at the single-cell level. mRNA levels of MEF-2 isoforms were assessed in the indicated HTLV-1-infected and uninfected cell lines using the PrimeFlow™ RNA assay according to the manufacturer's protocol. Cells were surface stained for anti-CD4 (PerCP Cy5.5) and individually hybridized with either an RPL13A probe (Alexa Fluor 488) to gate for transcriptionally active cells, or one of the four MEF-2 isoform probes (Alexa Flour 647 conjugated). Following target hybridization, signal amplification is accomplished through serial and sequential hybridizations of the highly specific Preamplifier molecules, which only hybridize when both sides of the target probe pair are bound to the target RNA. Upon completion of the assay, the cells were analyzed using BD FACS Calibur (BD Biosciences). MEF-2 mRNA levels were also evaluated by RT-qPCR to validate PrimeFlow™ results. RNA was converted into cDNA, which was then used as a template for qPCR amplification with primers given in (Supplemental Table 1). The fold-change expression was normalized to Jurkat and calculated by $2^{-\Delta\Delta CT}$ method. Total RNA from patient samples was converted to cDNA and amplified using standard real-time PCR. Fold-change expression was normalized to activated PBMCs.

MEF-2 isoform protein detection by western blot and WES (Protein Simple). Western blotting was performed as described above utilizing MEF-2 isoform (A-D)-specific antibodies from Proteintech in the dilution of 1:1000. Automated quantitative protein analysis was performed

by WES (Protein Simple, San Jose, CA) according to manufacturer's instructions. Lysates were diluted to optimum concentration using Simple Western sample dilution buffer (ProteinSimple) mixed with the fluorescent master mix and denatured at 95°C for 3 mins. Samples, primary antibodies, and HRP-conjugated secondary antibodies were loaded in pre-assigned wells of a 25-sample cartridge, then placed in WES instrument (Protein Simple). Primary antibodies were titrated for WES and utilized in the dilution of 1:50 for MEF-2A, MEF-2B, MEF-2C, MEF-2D, and Vinculin (R&D Systems). After capillary-based separation of the protein samples and incubation with the primary and secondary antibodies, proteins were detected using chemiluminescence. Protein signal and quantitation was generated automatically after each run through the Compass for SW software. Detected protein quantities are presented as area under the curve, normalized to vinculin as a loading control.

To assess MEF-2 isoforms in the nuclear-cytoplasmic fractions, cells were collected, washed with PBS and then nuclear-cytoplasmic extracts collected using NucBuster™ Protein Extraction Kit (MilliporeSigma). After isolation of the cytoplasmic fraction, the cell pellet was sonicated along with reagent B and then supernatant was collected. Both the cytoplasmic and nuclear fractions were probed for MEF-2A, -2B, -2C, and -2D (Proteintech) along with GAPDH as the loading control by western blotting.

siRNA/miRNA transfection. We obtained SMART pool siRNA (a pool of 4 sequences of siRNAs) for each isoform of MEF-2A from Dharmacon (Cat**:** L-009362-00-0010) and MEF-2C (L-009455-00-0010), miR21C human (HMI 0372). Cells (3 x 10^5/well) were plated on 6-well plates and transfections were performed using Lipofectamine™ RNAiMAX (Invitrogen) according to manufacturer's protocol. Briefly, Lipofectamine™ and siRNA/miRNA were diluted in Opti-

MEM medium (Gibco). The diluted Lipofectamine™ and siRNA/miRNA were incubated in a 1:1 ratio for 15 mins at room temperature. The siRNA-lipid/miRNA-lipid complex was added to the corresponding wells. After 48 hrs. of incubation at 37°C, cell pellets were collected and processed to obtain total RNA (Qiagen RNAeasy mini kit) and protein, for RT-qPCR and western blotting, respectively.

Ki-67 and Propidium iodide staining. The representative cell lines were plated and subjected to siMEF-2A or siMEF-2C treatment at 25 nm concentration using Lipofectamine™ RNAiMAX (Invitrogen), along with negative scramble controls. The cells were collected 48 hrs post-transfection, washed with 1X PBS and cell pellets fixed with 2 mL of 70% ethanol overnight at -20°C. The cell suspension was resuspended with 20 μL of PE-KI-67 (BD Biosciences), mixed gently and incubated at room temperature for 30 mins. The cells were washed with 2 mL of staining buffer at 200xg for 5 mins and 500 μL of staining buffer was added to each tube and FACS analysis was performed. Cells were washed and RNase inhibitor and PI ready-probe reagent (Invitrogen) was added. The resulting DNA distributions were obtained by BD FACS Calibur (BD) and quantified for the proportion of cells in cell cycle phases using Flow-Jo software.

Chromatin immunoprecipitation (ChIP) and Co-IP assays. ChIP assays were performed using Pierce Magnetic ChIP Kit (Thermo Scientific) per manufacturer's instructions with modifications for non-adherent cells. Crosslinking and cell pellet isolation were performed using approximately $4x10^6$ cells per ChIP. Briefly, cells were pelleted and fixed with 16% formaldehyde in serum free media, quenched with 1x glycine and washed twice with 1x PBS. Steps for Lysis and MNase digestion, IP elution, and DNA recovery was performed per manufacturer's protocol.

Immunoprecipitation was adjusted and combined such that magnetic beads, target antibodies (Supplemental Table 2) and chromatin samples were incubated overnight at 4°C. Eluted DNA was then eluted and subjected to RT-PCR using primers listed in supplemental Table 3. Samples were normalized to IgG for fold enrichment or adjusted based on 10% input for analysis.

For Co-IP, cells were lysed by sonication and cells lysates were pre-cleared with protein L magnetic beads. Samples were incubated overnight with 2mg of indicated antibodies and were washed to remove beads. Immunoprecipitated samples were resolved by SDS-PAGE and immunoblotted for either HBZ antibody or Menin and probed for the indicated markers.

In vivo testing of MC1568 in NOD/IL-2Rγc null (NOG) mice. For leukemia, a humanized mouse model has been generated by the intra-bone marrow (IBM) injection of human $CD133^+$ stem cells into NOD/Shi-scid/IL-2Rγc null (NOG) mice (16). We adopted this model to test MC1568 effects in early HTLV-1 infection. Briefly, five-week-old female NOD/SCID/γ-null (NODC57/BL) mice were housed and treated in accordance with the Institutional Laboratory Animal Care and Use Committee. Each group had a total of 5 mice. Animals were irradiated within the first week of birth, receiving 10 million human $CD34^+$ cells, and then housed for 8-10 weeks. Once animals were at least 60% humanized, they received one interperitoneally injected dose of 10 million irradiated MT-2 cells. The animals were housed for another 2 weeks to allow for viral spread then stratified into vehicle control and treatment groups. After the 2-week incubation, animals were treated with MC1568 (5mg/kg) at Day 0 and Day 3. Animals were sacrificed 7 days post-MC1568 treatment. Splenocytes and PBMC were isolated for DNA/RNA isolation and assessment of proviral load as well as viral gene expression as described above for cell lines.

Supplementary Figure Legends.

Figure S1. Characterization of cell lines utilized. A) Viability of an uninfected control cell line (Jurkat) and 7 chronically HTLV-1-infected cell lines assessed by the MTT Cell Proliferation Assay. Results are expressed as mean percent viability ±SD of duplicate samples. B, C) Copy number of integrated HTLV-1 genome was determined based on qPCR amplification of the Px region. Left, a standard curve made with different concentrations of TARL-2 cell DNA (500, 250, 125 and 62.5 ng), which is known to have 1 copy of virus/cell. The unknown copy number of each cell line was then calculated by replacing the CT value duplicates in the standard curve formula, divided by the estimated number of cells in each well (1 ng DNA =151.51 diploid cells), being represented here on the right side as mean copy number per cell ±SEM. D) Expression of major viral proteins Tax and HBZ were quantified by western blot analysis. Cofilin was used as a loading control and data is representative of two independent experiments. E) Standard curve generated using two-fold serial dilutions of HTLV-1 antigen, ranging from 0 to 800 pg/mL (left). P19 concentration for each cell line was determined via HTLV p19 Antigen ELISA (Zeptometrix) and calculated from the standard curve. F) Bar graph represents mean p19 concentration (pg/mL) ±SEM of the duplicate samples G) Immunophenotyping of cell lines expressing $CD3^+/CD4^+$ and Tax. Cellular expression of $CD3^+/CD4^+$ and Tax were determined by flow cytometry. Roughly, 1×10^6 cells per sample were incubated with fluorochrome-conjugated antibodies for CD3 (AF700), CD4 (FITC), or Tax (APC). Unstained samples (blue peaks) were used to compare the fluorescence of antibody-stained samples (red peaks).

Figure S2. MEF-2 isoform expression via Prime Flow and Non-ATLL cell lines. A) RT-qPCR results were validated by flow cytometry of the final samples from the PrimeFlow™ RNA assay.

Data represents the percentage of each cell line expressing both CD4 and the indicated MEF-2 isoform as determined with PrimeFlow™ RNA assay (Affymetrix/eBioscience). B) RT-qPCR was performed to assess the expression of MEF-2 isoforms in non-ATLL cell lines. MEF-2 mRNA expression is presented as the mean fold-change of two independent experiments relative to uninfected, activated T cells, which is normalized to one. Error bars represent the standard deviation of duplicate samples.

Figure S3. Additional validation of knockdown of MEF-2A and MEF-2C via siRNA and miR-21c respectively. A) Immunoblots of Jurkat cells treated with siMEF2A/C at 10, 25 and 50nm. Virtual blots are representative of 3 independent experiments. B) Bar graph represents K/D of MEF2A/C in comparison to scrambled control in MT-2 cells. Following transfection, RT-qPCR conducted to assess the expression of MEF-2. MEF-2 isoforms, HBZ and Tax are also represented as fold-change compared to scrambled control. C) Knockdown of MEF-2C post miR-21C treatment was analyzed by rt-qPCR. D) Cells were stained with Ki-67 and subjected to flow cytometric assays to measure cellular proliferation and the knockdown of MEF-2C via miR-21C treatment. Dot plots represent the amount of proliferation as measured by Ki-67 staining. Analysis was carried out with Flow-Jo software to quantify the proliferation profiles for each cell line and represented as a bar graph. E) Jurkat, ATL-ED, and MT-4 cells were collected, fixed, and stained with propidium iodide (PI-25μg/ml) to assess cell cycle progression via flow cytometry. Left, Mock transfected. Right, si-MEF-2A (50nM) transfection. The percentage of sub-G1 cells, G0/G1, S and G2-M cells was analyzed using Flow-Jo software and represented as a stacked column plot.

Figure S4. RNA and protein expression of MEF-2 isoforms in patient derived immortalized cell lines. A) Patient-derived NA-ATLL cell lines were subjected to RT-qPCR to determine MEF-2 isoform expression as well as Tax and HBZ expression. Expression of MEF-2 isoforms was normalized to activated T cells and fold-change calculated in reference to activated T cells, along with the fold-change of viral genes Tax and HBZ. B) MEF-2A, MEF-2B, MEF-2C, Tax and HBZ protein expression was analyzed via western blot for all NA-ATLL cell lines. Cofilin was used as a loading control. C) MEF-2A and MEF-2C virtual blots and quantification of ATL-18 and ATL-21 in comparison with Jurkat cells.

Figure S5. A) ChIP analysis of ATL-ED cells for enrichment of transcriptional targets in the 5'LTR of the transcriptionally silent viral promoter. B) ChIP analysis of MT-4 cells for enrichment of transcriptional targets in the 5'LTR of the transcriptionally active viral promoter and 3'LTR and canonical MEF-2 promoter NR4A1.

Supplementary Tables.

Supplementary Table 1: List of primers used for qPCR.

Primer	Sequence (5' to 3')
Human HBZ, forward	CAGTAGGGCGTGACGATGTA
Human HBZ, reverse	TCTTCCTCCAAGGATAATAGCCCGTCCA
Human MEF-2A, forward	CCGACTGCCTACAACACTGA
Human MEF-2A, reverse	GATAACTGCCCTCCAGCAAC
Human MEF-2B, forward	AAGTTCGGGCTGATGAAGAA
Human MEF-2B, reverse	CATACTGGAAGAGGCGGTTG
Human MEF-2C, forward	CTGGCAACAGCAACACCTAC
Human MEF-2C, reverse	GAAGGCAGGGAGAGATTTG
Human MEF-2D, forward	CACCTGACAATCACCCACAC
Human MEF-2D, reverse	AGCATCACCATACAGCACGA
Human Px region (Tax), forward	CAAAGTTAACCATGCTTATTATCAGC
Human Px region (Tax), reverse	ACACGTAGACTGGGTATCCGAA
Human β-actin, forward	TGCTGCCATCGTAAACTGAC
Human β-actin, reverse	CTTCCACAGGGCTTTGTTTC

Supplementary Table 2: List of antibodies used.

Primary antibody	Company	Catalog number
MEF2A Rabbit Polyclonal antibody	Proteintech	12382-1-AP
MEF2B Rabbit Polyclonal antibody	Proteintech	18710-1-AP
MEF2C Rabbit Polyclonal antibody	Proteintech	10056-1-AP
MEF2D Rabbit Polyclonal antibody	Proteintech	14353-1-AP
Cofilin Rabbit Polyclonal antibody	Abcam	ab42824
Jun D Mouse monoclonal antibody	Santa Cruz	sc-271938
MEN1 Polyclonal antibody	Proteintech	15159-1-AP
CREB1 Rabbit Polyclonal antibody	Proteintech	12208-1-AP
PCAF Rabbit Polyclonal antibody	Proteintech	13983-1-AP
SIN3A Mouse Monoclonal antibody	Proteintech	67197-1-Ig
SP1 Rabbit Polyclonal antibody	Proteintech	21962-1-AP
SP3 Rabbit Polyclonal antibody	Proteintech	26584-1-AP
CEBPA Rabbit Polyclonal antibody	Proteintech	8311-1-AP
HDAC3 Rabbit Polyclonal antibody	Proteintech	10255-1-AP
HDAC4 Mouse Monoclonal antibody	Proteintech	66838-1-Ig
GAPDH Rabbit monoclonal antibody	Cell signalling	2118
NUR77 Rabbit Polyclonal antibody	Proteintech	12235-1-AP
Secondary antibody	**Company**	**Catalog number**
Rabbit anti-goat IgG (H+L), HRP conjugate	Proteintech	SA00001-4
Goat anti-mouse IgG (H+L), HRP conjugate	Proteintech	SA00001-1
Goat anti-rabbit IgG (H+L), HRP conjugate	Proteintech	SA00001-2

Supplementary Table 3: List of primers used for Chip-RT PCR.

Primer Sequence	Primer Name
CCCTCCCGCTGGTTATTC	NR4A1-F
GCGCGGATTGTTTGATCTATAA	NR4A1-R
GCCTCTCCTCCTACTTTTATGATG	5’ LTR primer F
ACCTTGGTCTCGTTTTCACT	5’ LTR primer R
GTGAGGGGTTGTCGTCA	3’ LTR primer F
AACGAAAAAGAGGCAGATGA	3’ LTR primer R

Supplemental References:

1. Haertle T, Carrera CJ, Wasson DB, Sowers LC, Richman DD, Carson DA. Metabolism and anti-human immunodeficiency virus-1 activity of 2-halo-2',3'-dideoxyadenosine derivatives. J Biol Chem. 1988 Apr 25;263(12):5870-5. Epub 1988/04/25. Cited in: Pubmed; PMID 3258602.

2. Harada S, Koyanagi Y, Yamamoto N. Infection of HTLV-III/LAV in HTLV-I-carrying cells MT-2 and MT-4 and application in a plaque assay. Science. 1985 Aug 9;229(4713):563-6. Epub 1985/08/09. Cited in: Pubmed; PMID 2992081.

3. Posch W, Piper S, Lindhorst T, Werner B, Fletcher A, Bock H, Lass-Florl C, Stoiber H, Wilflingseder D. Inhibition of human immunodeficiency virus replication by cell membrane-crossing oligomers. Mol Med. 2012 Feb 10;18:111-22. Epub 2011/11/23. doi:10.2119/molmed.2011.00128. Cited in: Pubmed; PMID 22105607.

4. Rowe T, Dezzutti C, Guenthner PC, Lam L, Hodge T, Lairmore MD, Lal RB, Folks TM. Characterization of a HTLV-I-infected cell line derived from a patient with adult T-cell leukemia with stable co-expression of CD4 and CD8. Leuk Res. 1995 Sep;19(9):621-8. Epub 1995/09/01. Cited in: Pubmed; PMID 7564472.

5. Arnold J, Zimmerman B, Li M, Lairmore MD, Green PL. Human T-cell leukemia virus type-1 antisense-encoded gene, Hbz, promotes T-lymphocyte proliferation. Blood. 2008 Nov 1;112(9):3788-97. Epub 2008/08/12. doi:10.1182/blood-2008-04-154286. Cited in: Pubmed; PMID 18689544.

6. Feuer G, Fraser JK, Zack JA, Lee F, Feuer R, Chen IS. Human T-cell leukemia virus infection of human hematopoietic progenitor cells: maintenance of virus infection during differentiation in vitro and in vivo. J Virol. 1996 Jun;70(6):4038-44. Epub 1996/06/01. Cited in: Pubmed; PMID 8648741.

7. Koeffler HP, Chen IS, Golde DW. Characterization of a novel HTLV-infected cell line. Blood. 1984 Aug;64(2):482-90. Epub 1984/08/01. Cited in: Pubmed; PMID 6331549.

8. Panfil AR, Al-Saleem J, Howard CM, Mates JM, Kwiek JJ, Baiocchi RA, Green PL. PRMT5 Is Upregulated in HTLV-1-Mediated T-Cell Transformation and Selective Inhibition Alters Viral Gene Expression and Infected Cell Survival. Viruses. 2015 Dec 30;8(1). Epub 2016/01/06. doi:10.3390/v8010007. Cited in: Pubmed; PMID 26729154.

9. Maeda M. Human T lymphotropic virus type-I (HTLV-I) immortalizes human T cells in vitro--its implication in the pathogenesis of adult T cell leukemia (ATL). Hum Cell. 1992 Mar;5(1):70-8. Epub 1992/03/01. Cited in: Pubmed; PMID 1419953.

10. Taniguchi Y, Nosaka K, Yasunaga J, Maeda M, Mueller N, Okayama A, Matsuoka M. Silencing of human T-cell leukemia virus type I gene transcription by epigenetic mechanisms. Retrovirology. 2005 Oct 22;2:64. Epub 2005/10/26. doi:10.1186/1742-4690-2-64. Cited in: Pubmed; PMID 16242045.

11. Ahsan MK, Masutani H, Yamaguchi Y, Kim YC, Nosaka K, Matsuoka M, Nishinaka Y, Maeda M, Yodoi J. Loss of interleukin-2-dependency in HTLV-I-infected T cells on gene silencing of thioredoxin-binding protein-2. Oncogene. 2006 Apr 6;25(15):2181-91. Epub 2005/11/30. doi:10.1038/sj.onc.1209256. Cited in: Pubmed; PMID 16314839.

12. Lavorgna A, Matsuoka M, Harhaj EW. A critical role for IL-17RB signaling in HTLV-1 tax-induced NF-kappaB activation and T-cell transformation. PLoS Pathog. 2014 Oct;10(10):e1004418. Epub 2014/10/24. doi:10.1371/journal.ppat.1004418. Cited in: Pubmed; PMID 25340344.

13. Choi YB, Harhaj EW. HTLV-1 tax stabilizes MCL-1 via TRAF6-dependent K63-linked polyubiquitination to promote cell survival and transformation. PLoS pathogens. 2014 Oct;10(10):e1004458. Epub 2014/10/24. doi:10.1371/journal.ppat.1004458. Cited in: Pubmed; PMID 25340740.

14. Tateno M, Kondo N, Itoh T, Chubachi T, Togashi T, Yoshiki T. Rat lymphoid cell lines with human T cell leukemia virus production. I. Biological and serological characterization. J Exp Med. 1984 Apr 1;159(4):1105-16. Epub 1984/04/01. doi:10.1084/jem.159.4.1105. Cited in: Pubmed; PMID 6323614.

15. Rahman S, Quann K, Pandya D, Singh S, Khan ZK, Jain P. HTLV-1 Tax mediated downregulation of miRNAs associated with chromatin remodeling factors in T cells with stably integrated viral promoter. PLoS One. 2012;7(4):e34490. Epub 2012/04/13. doi:10.1371/journal.pone.0034490. Cited in: Pubmed; PMID 22496815.

16. Tezuka K, Xun R, Tei M, Ueno T, Tanaka M, Takenouchi N, Fujisawa J. An animal model of adult T-cell leukemia: humanized mice with HTLV-1-specific immunity. Blood. 2014 Jan 16;123(3):346-55. doi:10.1182/blood-2013-06-508861. Cited in: Pubmed; PMID 24196073.

Supplementary Figure 1

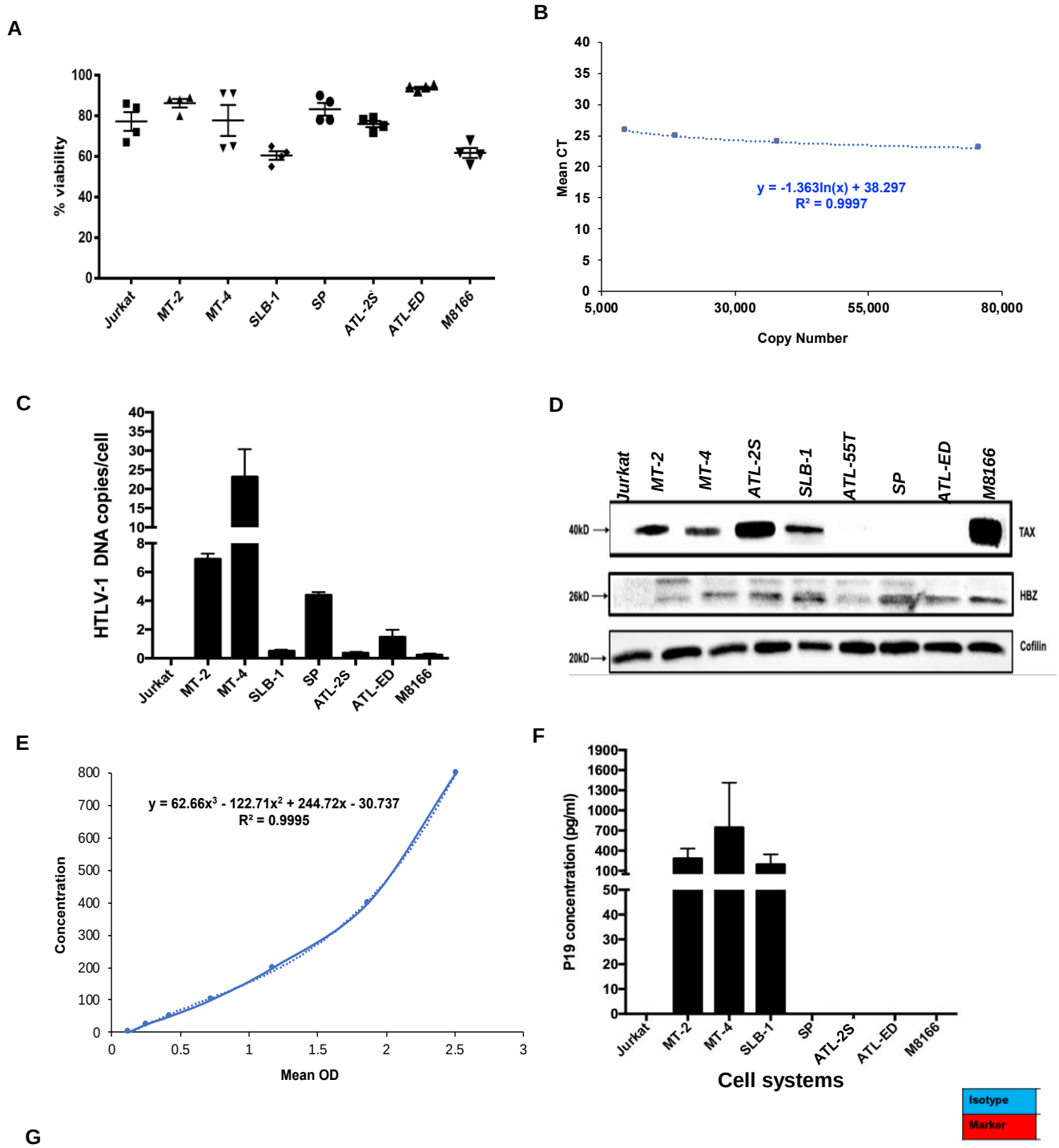

Supplementary Figure 2

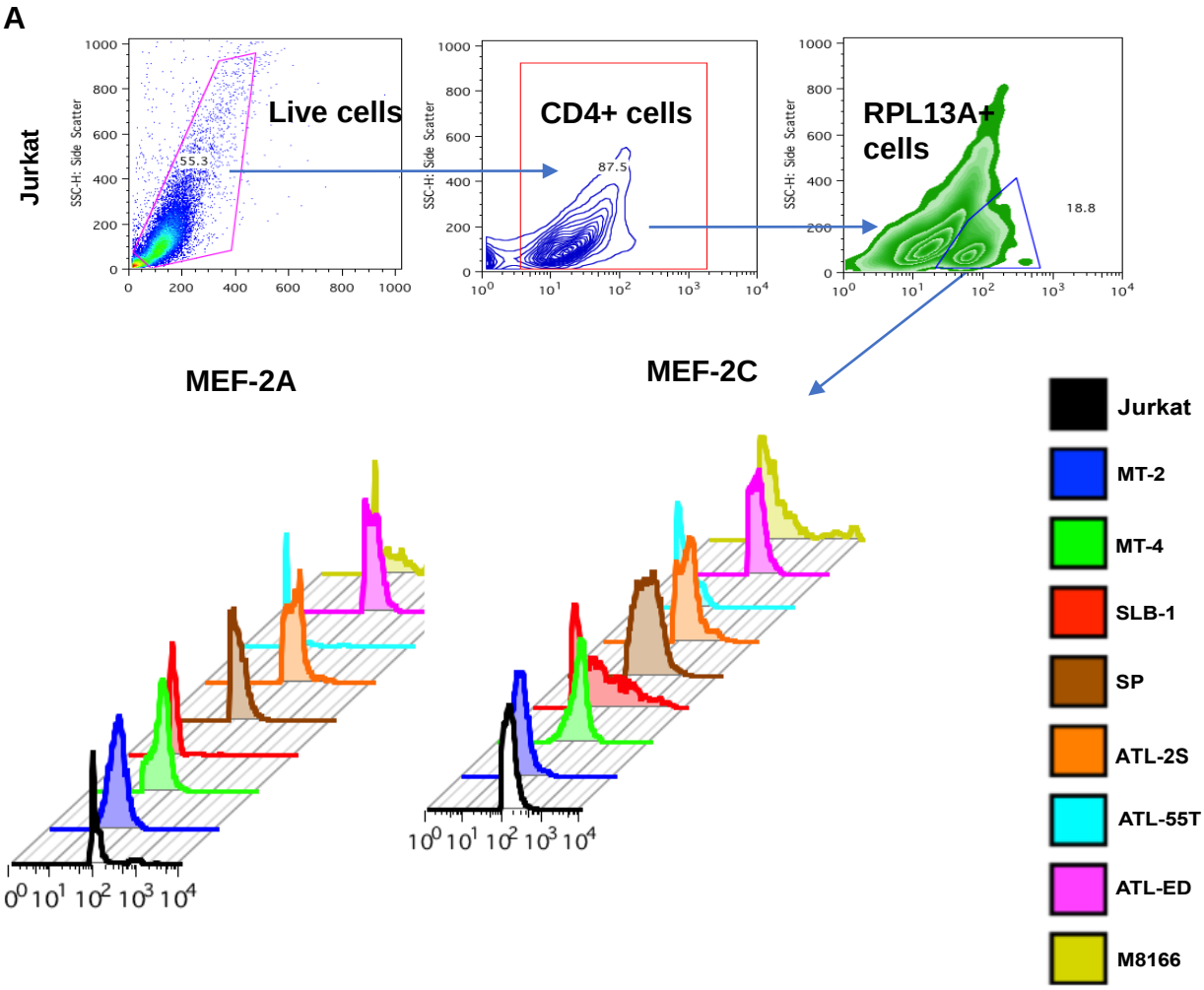

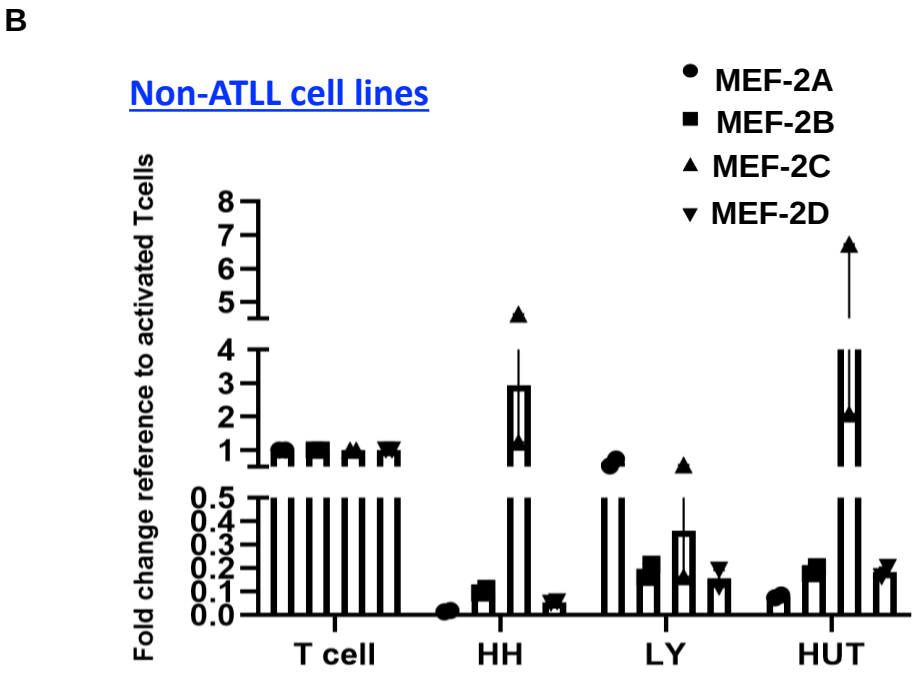

Supplementary Figure 3

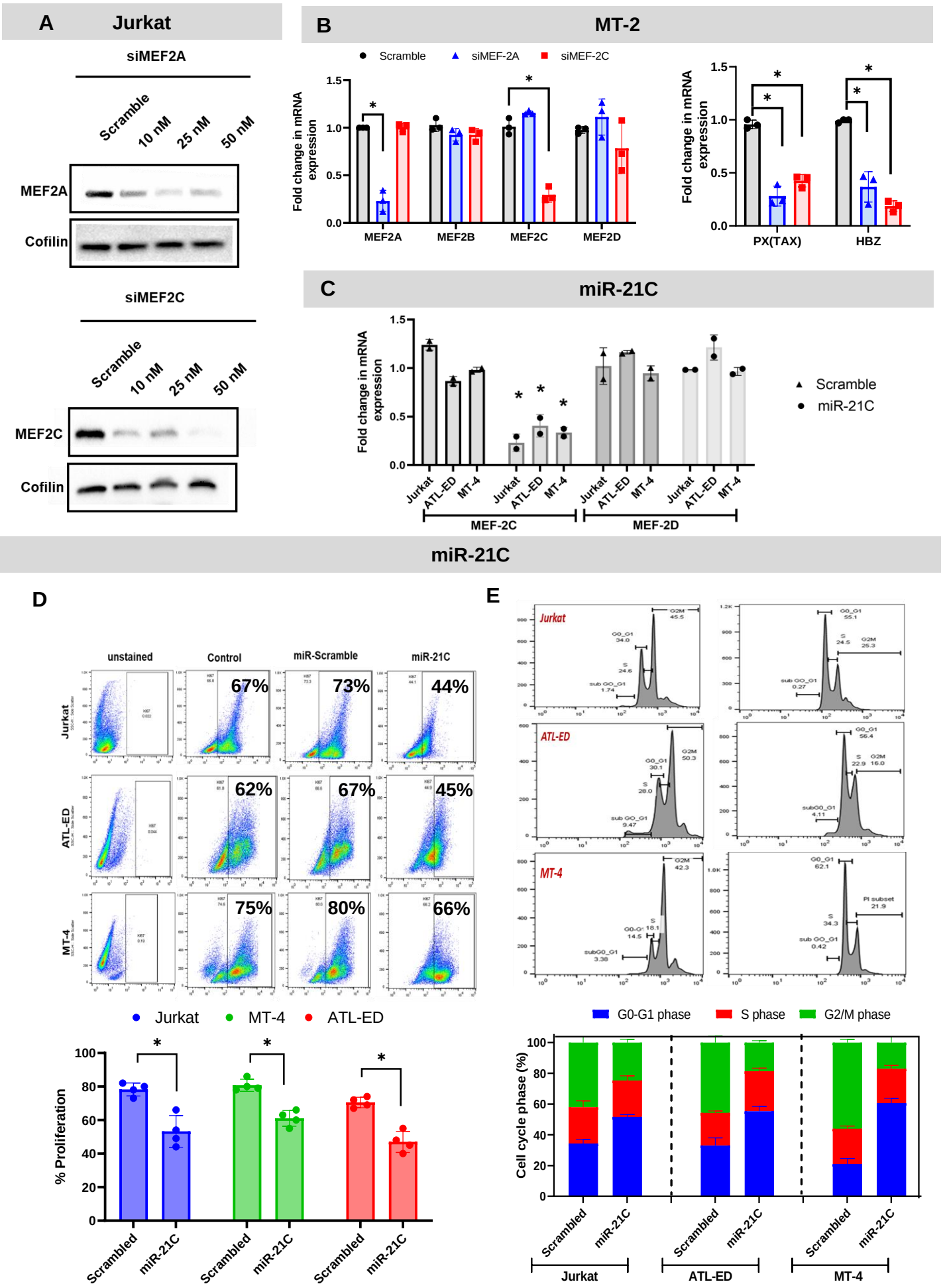

Supplementary Figure 4

A

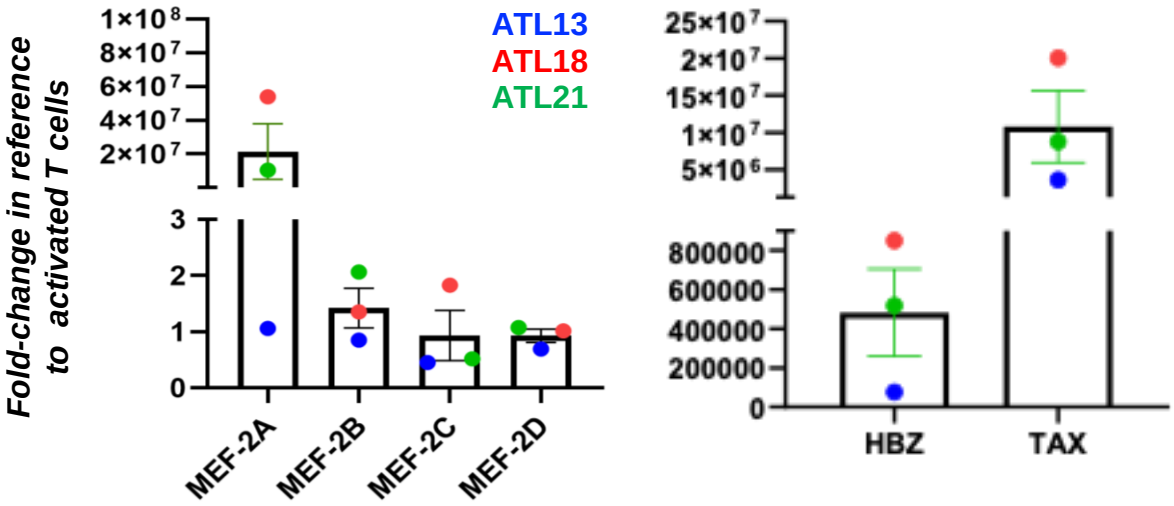

B

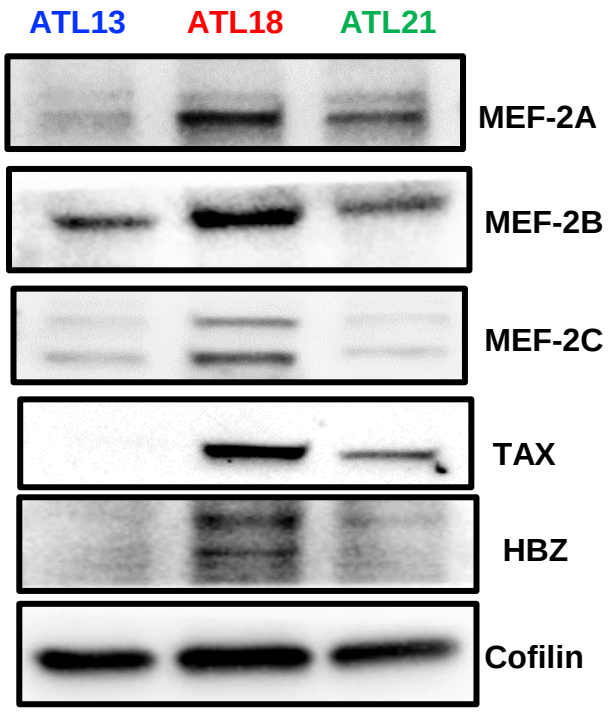

C

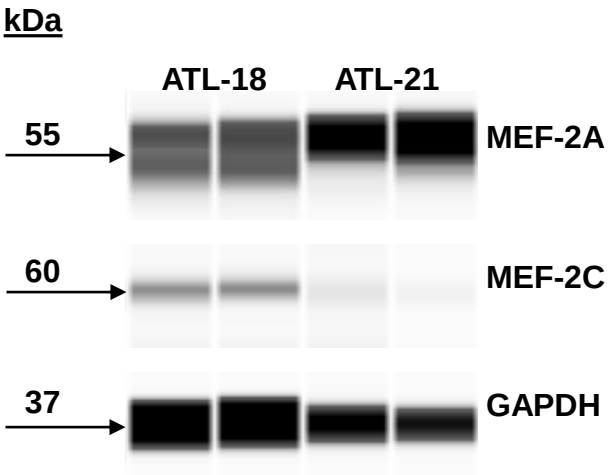

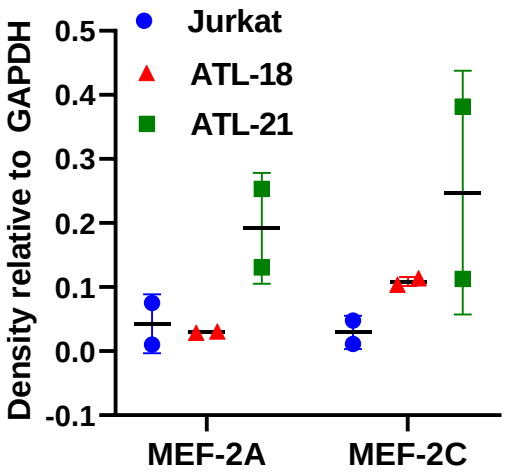

Supplementary Figure 5

A

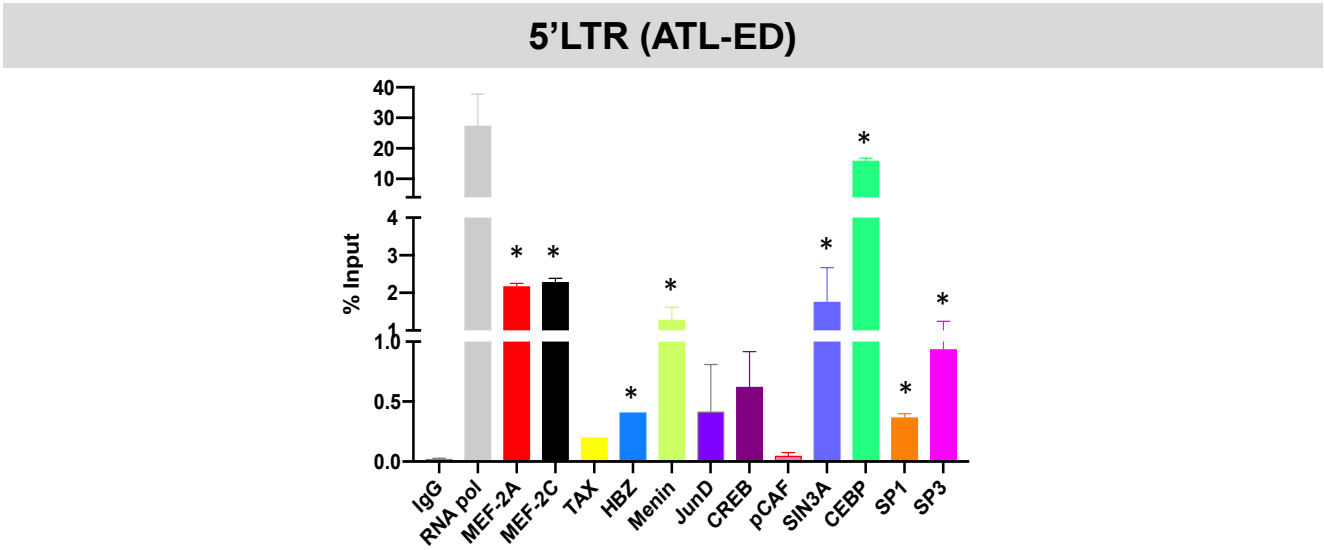

B